

1 **tDCS changes in motor excitability are specific to orientation of current flow**

2

3 Vishal Rawji¹, Matteo Ciocca¹, André Zacharia^{1,3}, David Soares¹, Dennis Truong², Marom
4 Bikson², John Rothwell¹, Sven Bestmann¹

5 ¹Sobell Department of Motor Neuroscience and Movement Disorders, UCL Institute of Neurology,
6 University College London, London, UK

7 ²Department of Biomedical Engineering, The City College of The City University of New York, New
8 York City, USA

9 ³Department of Neurology, University Hospitals of Geneva, Switzerland

10

11 **Corresponding author details**

12 Vishal Rawji

13 UCL Institute of Neurology,

14 London, WC1N 3BG, UK

15 Tel: +44 (0)20 3448 8758

16 Email: vishal.rawji.11@ucl.ac.uk

17

18

19 **Abstract**

20 Measurements and models of current flow in the brain during transcranial Direct Current
21 Stimulation (tDCS) indicate stimulation of regions in-between electrodes. Moreover, the cephalic
22 cortex result in local fluctuations in current flow intensity and direction, and animal studies suggest
23 current flow direction relative to cortical columns determines response to tDCS. Here we test this
24 idea by measuring changes in cortico-spinal excitability by Transcranial Magnetic Stimulation Motor
25 Evoked Potentials (TMS-MEP), following tDCS applied with electrodes aligned orthogonal (across) or
26 parallel to M1 in the central sulcus. Current flow models predicted that the orthogonal electrode
27 montage produces consistently oriented current across the hand region of M1 that flows along
28 cortical columns, while the parallel electrode montage produces none-uniform current directions
29 across the M1 cortical surface. We find that orthogonal, but not parallel, orientated tDCS modulates
30 TMS-MEPs. We also show modulation is sensitive to the orientation of the TMS coil (PA or AP), which
31 is through to select different afferent pathways to M1. Our results are consistent with tDCS
32 producing directionally specific neuromodulation in brain regions in-between electrodes, but shows
33 nuanced changes in excitability that are presumably current direction relative to column and axon
34 pathway specific. We suggest that the direction of current flow through cortical target regions
35 should be considered for targeting and dose-control of tDCS.

36

37

38 **Highlights**

- 39 • Direction of current flow is important for tDCS after-effects.
40 • tDCS modulates excitability between two electrodes.
41 • tDCS differentially modulates PA and AP inputs into M1.

42

43 **Keywords**

44 transcranial magnetic stimulation, transcranial direct current stimulation, primary motor cortex

45

46 **Abbreviations**

47 PA: postero-anterior, AP: antero-posterior, ML: medio-lateral, tDCS: transcranial direct current
48 stimulation, MEP: motor evoked potential, M1: primary motor cortex, TMS: transcranial magnetic
49 stimulation; AP-TMS-MEPs: motor evoked potentials elicited with anterior-posterior directed TMS;
50 PA-TMS-MEPs: motor evoked potentials elicited with posterior-anterior directed TMS

51 **Funding**

52 This research did not receive any specific grant from funding agencies in the public, commercial, or
53 not-for-profit sectors.

54

55 Introduction

56 To date, the majority of studies in humans using transcranial direct current stimulation (tDCS) to
57 modulate cortical function employ a bipolar electrode montage: one electrode is usually placed over
58 the target site and the other at a distance. So, for the hand area of motor cortex (M1), a large anode
59 is conventionally centred over the anatomical location of the “hand knob” of the precentral gyrus,
60 with a cathode over the contralateral orbit (1). This dosing strategy, based on canonical studies by
61 Nitsche, Paulus and colleagues on how the position of large electrodes influences population-
62 averaged modulation of TMS-MEPs (2-4), is now widely applied for targeting diverse cortical target
63 regions (5, 6) though rarely with consideration for nuanced dose response (7-11). Intra-cranial
64 recordings (12, 13) and clinical imaging (14, 15), supported by current flow models (16, 17) show
65 bipolar electrode montages produce current flow in brain regions between electrodes. Though
66 putative brain targets between electrodes have been considered (18-20), previous tDCS studies have
67 not systematically isolated the consequences of inter-electrode current flow.

68

69 The “inter-electrode” considerations provoke a second question. Animal studies in lissencephalic
70 animals indicate polarity specific (anodal/cathodal) excitability changes for current directed normal
71 to the cortical surface (2), which corresponds to current flow directed along the primary dendritic
72 axis of cortical pyramidal neurons (21, 22). In the human cephalic cortex, such controlled stimulation
73 cannot easily be achieved and the directions of current flow underneath an electrode are complex
74 (23, 24). The position of primary motor cortex in the anterior wall of the central sulcus suggests that
75 electrode montages that direct current flow perpendicular through this gyral wall (and thus
76 predominantly along the primary dendritic axis of cortical pyramidal neurons) may optimally
77 modulate corticospinal excitability (CSE). The second question we address here is therefore whether
78 there are differences in the effect of tDCS on CSE when current is oriented perpendicularly across,
79 compared with parallel to, the cortical surface at the level of the M1 hand area. To this end, we
80 positioned tDCS electrodes 3.5 cm anterior and posterior to the hand area of M1 to direct current
81 flow across the central sulcus (Figure 1). This means that depending on the position of the anode
82 and cathode, current will flow through M1 in anterior-posterior (AP-tDCS) or posterior-anterior (PA-
83 tDCS) direction, respectively. In a second condition, we positioned electrodes 3.5 cm medial and
84 lateral to the M1 hand area to direct current flow in parallel along the cortical surface of central
85 sulcus (Figure 1). We refer to this as medio-lateral tDCS (ML-tDCS). Motor-evoked potentials (MEPs)
86 elicited with TMS (TMS-MEPs) were used to access CSE changes after stimulation with these two
87 orthogonal tDCS orientations.

88 We also addressed a third question. The effects of TMS on motor cortex are well-known to be
89 directional (25, 26). TMS with a monophasic pulse that induces an electric current flowing from
90 approximately posterior to anterior across the central sulcus (perpendicular to the line of the
91 individual’s central sulcus at that point) evokes MEPs (PA-TMS-MEPs) that have a shorter latency and
92 lower threshold than stimulation with an anterior-posterior induced current (AP-TMS-MEPs). It is
93 thought that this is because the two directions of stimulation activate different sets of presynaptic
94 inputs to corticospinal neurones (21). Indeed, brain slice studies of tDCS established modulation
95 varies across afferent axonal pathways or varied orientation (24, 27). We therefore hypothesised
96 that any effects of tDCS across M1 might also be directionally selective, and that they would interact
97 in different ways with the direction of TMS used for eliciting MEPs. Specifically, using tDCS to direct
98 current perpendicular to the M1 hand area, we expected that stimulation with a posterior cathode
99 and anterior cathode (PA-tDCS) would influence MEPs evoked by PA and AP TMS in a different way
100 to tDCS applied with an anterior anode and posterior cathode (AP-tDCS).

101 **Methods**

102 *Participants*

103 22 healthy volunteers (17 male, 21 right handed) aged 21-44 (mean age 28.95, SD 6.14) participated
104 in this experiment. The study was approved by the UCL Ethics Committee and none had
105 contraindications to TMS or tDCS as assessed by a TMS/tDCS screening questionnaire.

106

107 *Current flow modelling*

108 Finite Element Method (FEM) models of tDCS were generated to predict electric field (E-field)
109 orientation along the motor cortex. High resolution T1 and T2 weighted MRI scans (GRE sequence,
110 TR = 1900ms, TE = 2.2 ms and SPACE sequence, TR = 3200 ms, TE = 402 ms respectively) were
111 previously collected and segmented using a combination of automated and manual segmentation
112 techniques (28). Automated segmentation algorithms derived from Unified Segmentation in SPM8
113 (29, 30) were combined with updated tissue probability maps and morphological filters (smoothing,
114 dilation, erosion) specifically developed for current flow modeling (31). Additional image masks (fat,
115 electrodes, gels) and regions of interest (M1) were segmented using manual and semi-manual tools
116 (Simpleware, Synopsys) to remove aliasing artifacts, incorporate gyri-precise detail, and position
117 stimulation electrodes along or across the hand regions of the motor cortex, as identified using
118 anatomical landmarks (32, 33). Adaptive tetrahedral meshes were generated using a voxel-based
119 algorithm (Simpleware, Synopsys) with multiple domains corresponding to different material
120 conductivities verified by intra-cranial recording (in S/m: Scalp 0.465, fat 0.025, skull 0.01, CSF 1.65,
121 Grey matter 0.276, White matter 0.126, Air 1e-15, electrode 5.99e7, gel 1.4) (12, 34, 35). Meshes
122 were imported into a FEM solver (COMSOL Multiphysics) where the Laplace equation for
123 electrostatics ($\nabla \cdot (\sigma \nabla V) = 0$) was solved as the field equation given a normal current density
124 boundary condition on the anode equivalent to 1mA, ground boundary condition on the cathode,
125 and insulation on all other external boundaries. Results were scaled linearly to match experimental
126 conditions when necessary. E-field orientation was visualized with surface arrows seeded evenly
127 along M1. Arrow colors corresponded to E-field normal ($n \cdot E$) to the cortical surface. By convention,
128 positive normal E-field represented inward “anodal” E-field (red) while negative normal E-field
129 represented outward “cathodal” E-field (blue). Streamlines representing current flow through M1
130 were generated by seeding 100 points randomly along the surface of M1 and the gel-skin contact.
131 Current density was then traced throughout the model. Line thickness was a logarithmic function of
132 current density magnitude and colorized to Voltage (red, anode; blue, cathode).

133

134 *EMG Recordings*

135 Throughout the experiment, subjects were seated comfortably in a non-reclining chair, with their
136 right hand rested on a cushion. Electromyographic (EMG) activity was recorded from the right first
137 dorsal interosseous (FDI) muscle using Ag/AgCl cup electrodes arranged in a belly-tendon montage.
138 The raw signals were amplified and a bandpass filter was also applied. (20Hz to 2kHz (Digitimer,
139 Welwyn Garden City, UK)) Signals were digitised at 5kHz (CED Power 1401; Cambridge Electronic
140 Design, Cambridge, United Kingdom) and data were stored on a computer for offline analysis (Signal
141 Version 5.10, Cambridge Electronic Design, UK was used).

142

143 *Transcranial Magnetic Stimulation*

144 Single pulse TMS was employed using a Magstim 200² stimulator (The Magstim Co. Ltd) connected
145 via a figure-of-eight coil with an internal wing diameter of 7cm. The hotspot was identified as the

146 area on the scalp where the largest and most stable MEPs could be obtained for the right FDI
147 muscle, using a given suprathreshold intensity. The coil was held approximately perpendicular to the
148 presumed central sulcus and held tangentially to the skull with the coil handle pointing backwards
149 for postero-anterior (PA) stimulation and handle pointing forwards for antero-posterior (AP)
150 stimulation. A coloured pencil was used to draw the boundaries around the coil so that it could be
151 accurately positioned to the hotspot for further recordings, for PA and AP coil orientations.

152

153 *Transcranial Direct Current Stimulation*

154 Transcranial direct current stimulation (tDCS; Starstim, Barcelona; 1 mA) was applied via 3.14 cm²
155 Ag/AgCl gelled electrodes yielding an average electrode current density of 0.318 mA/cm². The
156 stimulation was applied for a total of 10 min, ramped up and down for five seconds at the beginning
157 and end of the stimulation. Participants were asked to stay awake and at rest during the stimulation.
158 Sham stimulation involved ramping up then down both at the start and end of the 10 min period,
159 with zero stimulation for the remaining time.

160 TDCS electrodes were positioned 3.5cm anterior and posterior to the TMS hotspot along the
161 orientation of the TMS coil; two further electrodes were placed 3.5cm medial and lateral to the
162 hotspot perpendicular to the coil orientation (i.e. along the length of the central sulcus). We note
163 that this convention is with regards to the approximate orientation of the central sulcus, which is
164 generally oriented at about 45 degrees with respect to the midline. For simplicity, we will assume
165 that this corresponds to the anterior-posterior and medio-lateral orientation of the brain.

166 Stimulation was set up remotely on a computer and delivered via a Bluetooth receiver connected to
167 the electrodes. We refer to stimulation with a posterior anode and anterior cathode as PA-tDCS, to
168 indicate the direction of the electric field; AP-tDCS refers to stimulation with an anterior anode and
169 posterior cathode. We refer to stimulation with a medial anode and lateral cathode (directing
170 current flow approximately in parallel to the central sulcus) as ML-tDCS (see Figure 2).

171

172 *Experimental Parameters*

173 Resting motor threshold (RMT) was defined as the lowest TMS stimulus intensity to evoke a
174 response of 50 μ V in 5 out of 10 trials in the relaxed FDI using the optimal PA orientation.

175 Twenty MEPs were collected before and after tDCS, with post tDCS MEPs collected every ten
176 minutes from T0-T40. The TMS stimulus intensity was set at the intensity required to evoke a
177 response of 1 mV peak-to-peak amplitude (SI1mV), and this intensity was kept constant throughout
178 the entire experiment. The mean amplitude of these MEPs was calculated for each time point for
179 each subject.

180

181 *Experiment 1*

182 In experiment 1, we investigated whether corticospinal excitability could be modulated with an
183 electrode montage for which the region of interest (M1 hand region) was positioned between our
184 stimulating electrodes. This was accomplished using two different stimulating montages, PA and ML
185 tDCS (as described above), to investigate whether direction of current flow across M1 could
186 differentially modulate responses. To this end, fifteen people participated in a crossover study,
187 which consisted of three randomised sessions (ML-tDCS, PA-tDCS and sham), each separated by at
188 least five days. MEPs were assessed before and after tDCS using PA TMS.

189

190 *Experiment 2*

191 Following the interesting results from experiment 1, we next asked whether the observed effect of
192 PA-tDCS on corticospinal excitability might be explained by specific modulation of posterior-to-
193 anterior or anterior-to-posterior inputs into M1, as probed by exploiting the known directional
194 sensitivity of TMS over M1. Fourteen people participated in this experiment. PA-tDCS was applied
195 and the effects on PA-TMS-MEPs and AP-TMS-MEPs were assessed. For each TMS stimulus direction
196 at each time point, 20 MEPs were acquired.

197

198 *Experiment 3*

199 To complete the permutations, we finally assessed the effect of AP-tDCS on both PA and AP TMS
200 pulses in the same group as in experiment 2.

201

202 **Data Analyses**

203 The amplitude of each single MEP at each time point was measured and averaged in each individual.
204 Data from each individual was then averaged into a grand mean and entered into a two-way
205 repeated measures analyses of variance (rmANOVA) with main factors “STIMULATION” (in
206 experiment 1: ML-tDCS, PA-tDCS and Sham) or “COIL DIRECTION” (PA and AP TMS coil orientations
207 in experiments 2 and 3) and “TIME” (Baseline, T0, T10, T20, T30 and T40 for all experiments).
208 Absolute MEP values were used in each statistical test. In cases where there was a significant
209 “STIMULATION” x “TIME” OR “COIL DIRECTION x TIME” interaction, analysis showed no overall effect
210 of TIME from T0-T40 (i.e. post-tDCS). Therefore we calculated the mean post-tDCS effect and
211 expressed this as a fraction of the baseline for post hoc testing. To examine test-retest reliability
212 between individuals having repeated PA-tDCS sessions, we used a (2,k) intraclass correlation
213 coefficient.

214

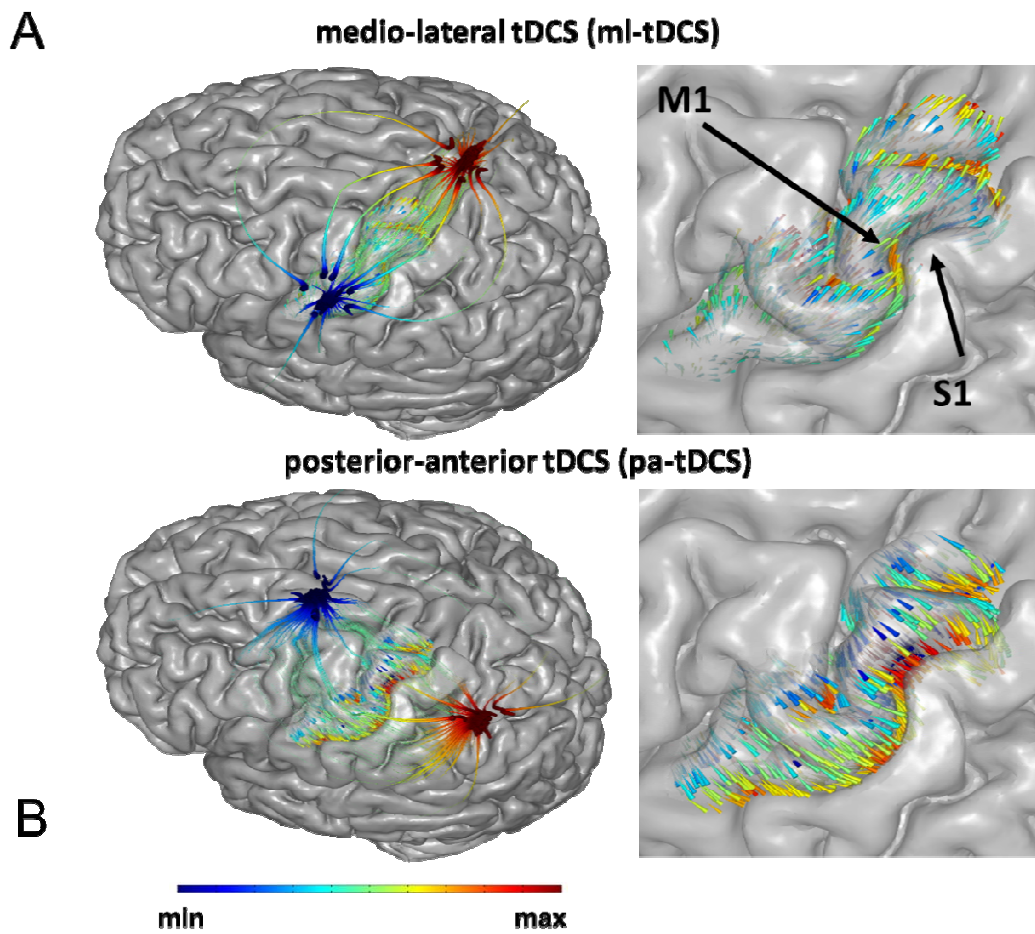
215

216

217 **Results**

218 *Modelling Current Flow*

219 The electrode montages we used have not been explored in detail previously. Adapting models with
220 parameters previously validated by intra-cranial recording (13), we calculated the expected electric
221 field distribution in the central area of the cerebral cortex using the electrodes and stimulation sites
222 in the present study. Figure 1 shows the predictions for ML-tDCS (top) and PA-tDCS (bottom). As
223 reported by others (17, 31, 36, 37), the modelling shows that with bipolar montages substantial
224 current flow (field intensities) are produced between the two electrodes. There is a notable and
225 clear difference between the two electrode montages: whereas ML-tDCS does not produce any
226 uniformly directed electrical fields through the surface of motor cortex, PA-tDCS leads to relatively
227 uniform inward and outward electrical fields, which are perpendicular relative to the cortical surface
228 of M1. For AP-tDCS the current directions reverse (not shown). Based on data from animal models
229 (22), inward and outward electric fields would correspond to preferential pyramidal soma
230 depolarization and hyper-polarization, respectively. For ML-tDCS, the direction of the electric field is
231 predominantly parallel long the cortical surface in central sulcus, which would suggest no dominant
232 pyramidal soma polarization polarity. A following prediction would be that electrode montages that
233 lead to relatively uniform electrical fields directed perpendicular to the cortical surface in M1 should
234 be more efficient in modulating CSE.



235

236

237 **Figure 1. Comparison of electrical field modelling for montages directing current**
238 **across and along the cortical surface**

239 Electric field orientation on the cortex as applied by electrodes along (A) or across (B)
240 the motor strip. Note: The streamlines and arrows have two separate colorscales.
241 Starting outside the motor-strip, streamlines trace the direction of current density from
242 high to low voltage (red to blue), anode to cathode. The streamlines confirm that
243 current flows down the voltage gradient established by the electrodes and shaped by
244 the head anatomy. On the motor strip, arrows illustrate the direction of electric field
245 passing through the motor cortex surface. Arrow colour represents normal electric field
246 where red is inward and blue is outward. Inward field corresponds to expected
247 pyramidal soma depolarization and outward corresponds to expected pyramidal soma
248 hyper-polarization (though we note that the polarization of axons and terminals must
249 also be considered). It is important to not confuse the red/blue of voltage with the
250 red/blue of electric field/polarization since the two are not simply related; none-the-
251 less, this representation allows correlation of macro-scale current flow patterns set by
252 electrode montage with gyri-scale current flow pattern which determine cellular
253 polarization. These modelling results show how current can be directed to flow more
254 uniformly through M1.

255

256
257 *Physiological Measurements*

258 No significant differences were found between TMS thresholds or amplitudes of the test MEP across
259 sessions. As expected AP TMS thresholds were higher than those for PA stimulation (see Table 1).

260

261 *PA- versus ML-tDCS: effects on PA-TMS-MEPs*

262 15 individuals were given 10 min of 1 mA tDCS using each of three separate tDCS montages tested in
263 separate sessions at least one week apart: PA-tDCS, ML-tDCS or sham-tDCS. MEPs were evaluated at
264 rest before and up to 40 min after tDCS (Figure 2A). PA-tDCS decreased the amplitude of MEPs
265 whereas there was no effect of either sham or ML-tDCS. This was confirmed in a two-way repeated
266 measures ANOVA with STIMULATION (PA, ML, sham) and TIME as main factors which showed a
267 significant STIMULATION x TIME interaction ($F(10, 140) = 1.991$; $p = 0.039$, $\eta^2 = 0.125$) indicating that
268 MEPs were affected differently by each type of tDCS. In order to understand the source of the
269 interaction, the mean post-tDCS effect has been expressed as a fraction of the baseline in Figure 2B.
270 A one way ANOVA showed a significant effect of type of STIMULATION ($F(2, 28) = 7.134$; $p = 0.002$,
271 $\eta^2 = 0.311$), with posthoc (Bonferroni corrected) paired t-tests and effect sizes showing a significant
272 difference between the effect of PA-tDCS and sham ($t = -3.279$; $p = 0.005$; $d = -1.110$) and PA v. ML-
273 tDCS ($t = -3.196$; $p = 0.006$) but not between sham and ML-tDCS ($t = 0.760$; $p = 0.46$; $d = 0.302$).

274

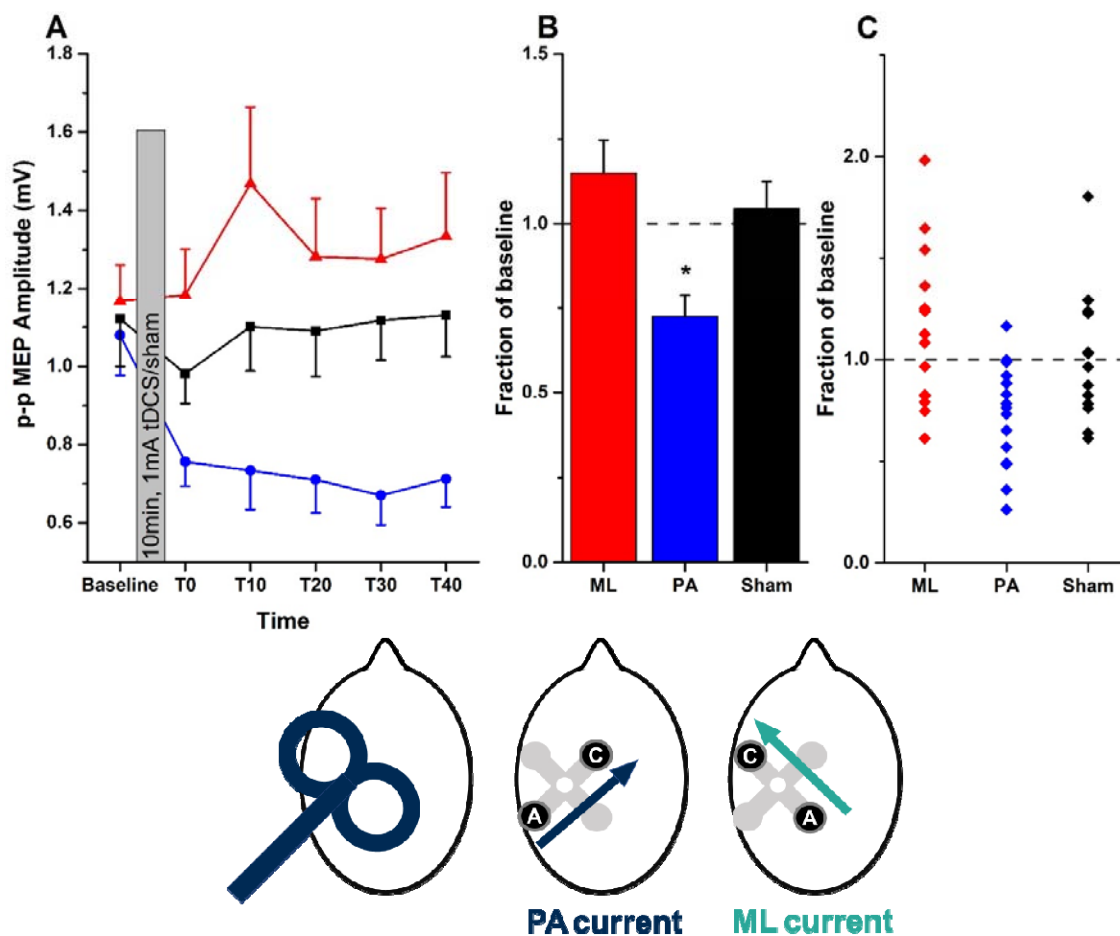


Figure 2. Effect of PA- and ML-tDCS on the amplitude of MEPs evoked by PA-TMS-MEPs.

A, mean (\pm SEM) MEP amplitudes at baseline and every 10 minutes between T0 and T40 (red triangles = ML-tDCS, black squares = Sham, blue circles = PA-tDCS). **B**, mean (\pm SEM) post-stimulation effect (averaged from T0 to T40) expressed as a fraction of the baseline value in each group (ML, red; PA, blue; sham, black). Asterisks represent paired t-test significant differences ($p < 0.05$ with Bonferroni's multiple correction) when compared to sham. **C**, individual data points contributing to the mean values plotted in B. The head diagrams represent coil orientation and electrode configuration used: PA-TMS-MEPs, PA-tDCS and ML-tDCS.

PA-tDCS: contrasting effects on PA- and AP-TMS-MEPs

We next examined in 14 participants whether PA-tDCS had different effects on the MEPs evoked by TMS directed in AP or PA fashion (ie. the coil handle pointing forward or backward). Baseline MEPs to each direction of TMS had the same amplitude (AP-TMS-MEPs: $0.983\text{mV} \pm 0.201$ vs PA-TMS-MEPs: $1.042\text{mV} \pm 0.226$), although the absolute intensity required for AP-TMS-MEPs ($49.1 \pm 2.6\%$) was higher than for PA-TMS-MEPs ($62.9 \pm 2.8\%$). Collapsing all the post-tDCS MEPs and expressing them as a fraction of the baseline (Figure 3A) revealed a significant effect of PA-tDCS on PA-TMS-

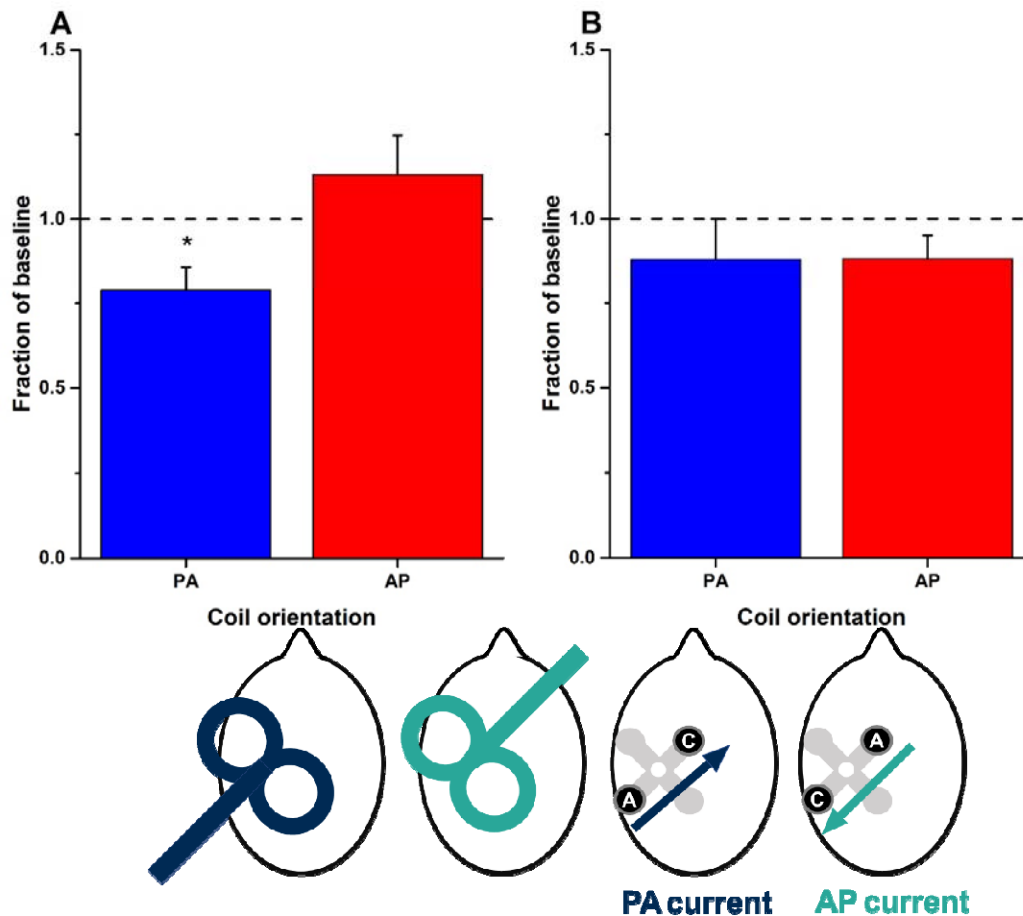
296 MEPs ($t = -2.73$; $p = 0.017$, $d = -0.980$) but no effect on AP-TMS-MEPs. There was a significant
297 difference in the effect on PA-TMS-MEPs vs AP-TMS-MEPs ($t = -2.565$; $p = 0.024$, $d = -0.946$).

298

299 *AP-tDCS: contrasting effects on PA- and AP-TMS-MEPs*

300 Given the equivocal effects of PA-tDCS on AP-TMS-MEPs (experiment 2), we finally tested whether
301 more consistent effects might be observed on AP-TMS-MEPs when AP-tDCS was employed. In the
302 same participants as in experiment 2 we compared the effects of AP-tDCS on PA-TMS-MEPs and AP-
303 TMS-MEPs (Figure 3B). Collapsing all the post-tDCS MEPs and expressing them as a proportion of the
304 baseline, post hoc paired t-tests revealed that there was no difference in the effect of AP-tDCS on
305 MEPs evoked by the two coil orientations ($t = -0.112$; $p = 0.913$, $d = 0.035$) nor were the MEPs to
306 either type of stimulation changed in size after AP-tDCS (Figure 3B).

307



308

309

310 **Figure 3. Effect of PA-tDCS (A) and AP-tDCS (B) on the amplitude of MEPs evoked**
311 **by PA- and AP-TMS-MEPs.**

312 Graphs plot overall mean (\pm SEM) post-stimulation effects (averaged from T0 to T40 and
313 expressed as a fraction of baseline values) for PA- (blue bars) and AP-TMS-MEPs (red
314 bars). Asterisks represent significant differences between the two coil orientations
315 ($p < 0.05$ with Bonferroni's multiple correction). The head diagrams represent coil

316 orientation and electrode configuration used: PA- and AP-TMS-MEPs, and PA- and AP-
317 tDCS.

318

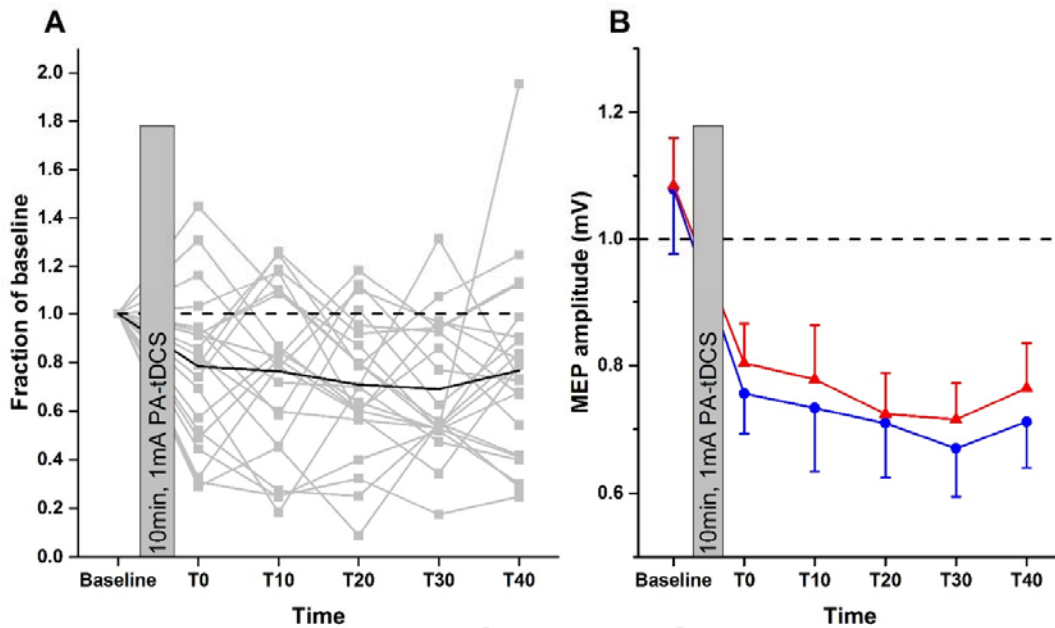
319

320 *Variability in responses to PA-tDCS*

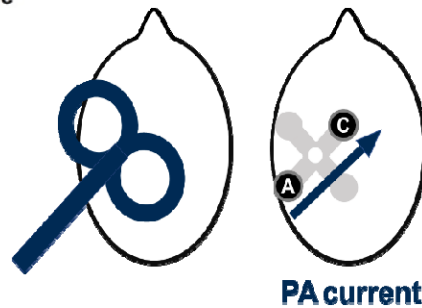
321 In total, 22 different individuals were examined for the effects of PA-tDCS on PA-TMS-MEPs. The
322 results for all of them are plotted in Figure 4A to illustrate the variability of the effect. Averaging
323 over all post-tDCS time points gives a mean reduction of the MEP to $74.3 \pm 5.1\%$ of baseline values.

324 In addition, 15 of these participants were tested on two separate occasions. The mean data from
325 session 1 and 2 are shown in Figure 4B. A two-way ANOVA showed no effect of SESSION ($p=0.2$, $F(1,$
326 $14) = 1.808$; $p = 0.2$, $\eta^2 = 0.028$) and no SESSION*TIME interaction ($F(5, 70) = 0.555$; $p = 0.70$, $\eta^2 =$
327 0.223) indicating no significant differences between the two sessions. There was however, a main
328 effect of TIME ($F(5, 70) = 7.328$; $p = 0.017$, $\eta^2 = 0.630$). The interclass correlation coefficient for the
329 mean percentage reduction in MEP was 0.68, which is generally classified as moderate-strong
330 reproducibility.

331



332



333

334 **Figure 4. A, inter-individual variation in the effect of PA-tDCS; B, repeatability of**
335 **group mean response to PA-tDCS on the amplitude of MEPs evoked by PA-TMS-**
336 **MEPs.**

337 **A**, In all 22 individuals, MEPs evoked at each post-TDCS time point have been expressed
338 as a fraction of baseline. The solid black line represents the average response from all
339 individuals. **B**, mean (\pm SEM) amplitudes at baseline and every 10 minutes, post-tDCS in
340 a group of 15 participants who were tested on 2 separate occasions (red and blue
341 symbols and lines). The head diagrams represent coil orientation and electrode
342 configuration used: PA-TMS-MEPs and PA-tDCS.

343

344

345

346 Discussion

347 Selecting the scalp position of electrodes relative to a brain target is a paramount consideration in
348 tDCS (5) – the common bipolar montage places one electrode over the target and the second
349 electrode at some distance. Motivated by previous studies (see below) and specific modelling
350 predictions (Figure 1), the present study shows that bipolar tDCS produces quantifiable changes in
351 the excitability of primary motor cortex when it is located between the positions of the two
352 stimulation electrodes, as opposed placing one electrode over M1. For the hand area, the effects on
353 corticospinal excitability depends also on the direction of the electric field: in line with the
354 predictions from current modelling, a montage orthogonal (perpendicular) to the gyrus generated
355 consistently directed electric fields as compared with a montage along (parallel) to the gyrus. This
356 was reflected in the after-effects on MEPs: they were suppressed after delivering perpendicular
357 current but there was no effect after parallel current. Finally, the direction in which tDCS was applied
358 across the sulcus (i.e. anode anterior or posterior) interacted differentially with the direction of TMS
359 pulses: PA-tDCS affected PA-TMS-MEPs, but had no effect on AP-TMS-MEPs. AP-tDCS had no
360 significant effect on either direction of TMS.

361

362 *Stimulation between two electrodes*

363 Previous modelling studies have predicted bipolar tDCS will produce cortical electric fields between
364 the two stimulation sites which may be as large or larger than those immediately under the
365 electrodes (17, 38, 39) – predictions recently validated (13, 40, 41). Moreover, our own modelling
366 presented here suggests that perpendicular current flow through the sulcus produces more
367 uniformly directed current at the target site, compared to montages that direct current along the
368 sulcus. This leads to the prediction that tDCS of M1 hand area will have different effects when
369 current is passed between electrodes posterior and anterior to the axis of the central sulcus,
370 compared with electrodes placed medial and lateral. These predictions were indeed borne out by
371 the present results: PA-tDCS leads to aftereffects on corticospinal excitability whereas ML-tDCS has
372 no effect. This also indicates that not just the strength of current but also its direction with regards
373 to the cortical surface play an important role in mediating changes in corticospinal excitability.

374

375 Although it is possible that the posterior anode changes activity in parietal cortex and this
376 secondarily leads to changes in M1, previous work suggests that electrodes positioned more
377 posteriorly do not effectively modulate corticospinal excitability (36). We conclude that stimulation
378 of sites between two scalp electrodes occurs with bipolar tDCS, as dictated by the physics of current
379 flow, which has important implications for studies seeking to target a specific brain region.
380 Moreover, our results indicate that controlling for the direction of current flow through a target
381 region may help to improve the efficacy of tDCS. For example, it is conceivable that in many studies a
382 mix of PA and ML currents will occur between subjects. If one adds to this the notion that the
383 intensity of stimulation will vary greatly across subjects when controlling stimulator output rather
384 than effectively applied current inside the brain (42, 43), we have the situation of large variability in
385 applied current intensity and direction at the presumed target site. Indeed, given our results, in
386 which ML-tDCS produced no reliable effects on CSE, such a mix of current flow direction may
387 contribute to reports of inter-subject variability in physiological and behavioural stimulation
388 outcomes (44-47). At least for motor cortex, control of current flow direction could be easily
389 achieved based on the optimal orientation and position of TMS for eliciting motor-evoked potentials.

390

391 *Directionality of tDCS directed across central sulcus*

392 “Anodal stimulation” with a large electrode placed directly over M1 can increase cortical excitability.
393 This is usually explained in the following way. Anodal stimulation produces an inward current flow
394 (18, 37), though not exclusively depending on cortical folding (24). Cortical pyramidal neurons,
395 including in M1, are aligned perpendicular to the surface of the cortex, such that an inward current
396 flow hyperpolarises their dendrites and depolarises the cell body (22). Neurophysiological studies in
397 animal indicate that the net effect of this is an increase in the excitability of the neuron (48, 49)
398 including to synaptic inputs (24), favouring build-up of an LTP-like effect over the 10 min of tDCS (2,
399 50). This is thought to result in larger MEPs when the same inputs are activated using TMS.

400 The current flow modelling work presented here shows that similarly directed tDCS produces
401 directional current which, depending on the polarity, enters and exits from the posterior and
402 anterior banks of the precentral gyrus. For PA-tDCS, inward flow on the anterior bank of the central
403 sulcus should polarise the pyramidal neurones in the sulcal wall (which are oriented parallel to the
404 surface of the brain) in the same way as direct “anodal stimulation” over M1 is presumed to operate
405 (though we note this inference stems from animal studies with well-controlled current flow). If so,
406 then we might expect that PA-tDCS has the same effect as conventional anodal tDCS. In fact, the
407 opposite was observed here: 10 min of 1 mA PA-tDCS suppresses MEPs, whereas “anodal
408 stimulation” directly over M1 enhances MEPs, despite this effect also being variable (44).

409 The different excitation by “anodal tDCS” applied with conventional or focal 4x1 HD electrodes (51),
410 and inhibition by PA-tDCS may be explained by difference in which neuronal elements are
411 modulated. In contrast to the above proposed action on cortical neurons in the gyri-wall by PA-tDCS,
412 “anodal tDCS” may modulate TMS responses by polarisation of cortical neurons specifically in gyral
413 crowns, where inward direct current is indeed more likely (24). PA-tDCS will produce current at the
414 gyri-crown parallel to the cortical surface, which is orthogonal to cortical neurons but aligned with
415 cortico-cortical axons afferents. This leads to an alternative hypothesis where PA-tDCS modulates
416 TMS response by polarisation of afferent axons in the gyri crown, which are sensitive to direct
417 current. Animal neurophysiology suggests direct current orientation toward the activated axon
418 terminal (PA in this case) will indeed decrease excitability (24, 27).

419 A range of further alternative explanations can be proposed, that to varying extents explain the lack
420 of the expected modulation of directional tDCS on changes in PA-TMS-MEPs or AP-TMS-MEPs. Even
421 using HD electrodes, tDCS is not focal so net changes in motor excitability may reflect actions on other
422 cortical regions (24, 52). A non-trivial dependence on tDCS polarity was already known (8) and the
423 non-linear properties of neurons (53) and networks can produce preferential responses to one tDCS
424 polarity (54).

425 In general, the nuance in neuromodulation identified here derives from details of cortical folding and
426 cellular morphology. Given that AP-TMS-MEPs and PA-TMS-MEPs activate different inputs to
427 corticospinal output neurones (21) it is not unforeseen that AP-TMS-MEPs were unaffected by PA-
428 tDCS. The dependence on idiosyncratic anatomy (and gradation in coil positioning) may lead to inter-
429 individual variability that masks population effects for many conditions, and produce individual
430 variability.

431

432 *Variability*

433 We examined the after-effects of PA-tDCS on PA-TMS-MEPs in 22 individuals and found that in 15 of
434 them tDCS reduced corticospinal excitability by 10% or more. Furthermore, the ICC for repeated
435 assessments within an individual was 0.68. Both of these figures are higher than previously reported
436 for standard montage tDCS (55). It would need a larger study to power this comparison adequately,
437 but it could be that by aligning the tDCS to the individual best direction for PA-TMS-MEPs we

438 achieved an increased uniformity of electric field normal to the surface of M1 compared with a
439 single central anode.

440

441 *Conclusion*

442 We provide strong support for the notion that bipolar tDCS has effects on cortex between the
443 primary sites of stimulation, as predicted by models of current flow in the brain. Furthermore, these
444 effects can be directionally-dependent. These factors may be important when interpreting (and
445 comparing) results from conventional tDCS. More generally, our results indicate how current flow
446 models can guide electrode placement and motivate experimental questions concerning the key
447 factors for optimizing tES.

448

449 *References*

- 450 1. Nitsche MA, Paulus W. Excitability changes induced in the human motor cortex by weak
451 transcranial direct current stimulation. *The Journal of physiology*. 2000;527 Pt 3:633-9.
- 452 2. Bindman LJ, Lippold OC, Redfearn JW. The Action of Brief Polarizing Currents on the Cerebral
453 Cortex of the Rat (1) during Current Flow and (2) in the Production of Long-Lasting after-Effects. *The*
454 *Journal of physiology*. 1964;172:369-82.
- 455 3. Nitsche MA, Paulus W. Sustained excitability elevations induced by transcranial DC motor
456 cortex stimulation in humans. *Neurology*. 2001;57(10):1899-901.
- 457 4. Nitsche MA, Doemkes S, Karakose T, Antal A, Liebetanz D, Lang N, et al. Shaping the effects
458 of transcranial direct current stimulation of the human motor cortex. *Journal of neurophysiology*.
459 2007;97(4):3109-17.
- 460 5. Brunoni AR, Nitsche MA, Bolognini N, Bikson M, Wagner T, Merabet L, et al. Clinical research
461 with transcranial direct current stimulation (tDCS): challenges and future directions. *Brain*
462 *stimulation*. 2012;5(3):175-95.
- 463 6. Lefaucheur JP, Antal A, Ayache SS, Benninger DH, Brunelin J, Cogiamanian F, et al. Evidence-
464 based guidelines on the therapeutic use of transcranial direct current stimulation (tDCS). *Clinical*
465 *neurophysiology : official journal of the International Federation of Clinical Neurophysiology*.
466 2017;128(1):56-92.
- 467 7. Nitsche MA, Fricke K, Henschke U, Schlitterlau A, Liebetanz D, Lang N, et al. Pharmacological
468 modulation of cortical excitability shifts induced by transcranial direct current stimulation in
469 humans. *The Journal of physiology*. 2003;553(Pt 1):293-301.
- 470 8. Batsikadze G, Moliadze V, Paulus W, Kuo MF, Nitsche MA. Partially non-linear stimulation
471 intensity-dependent effects of direct current stimulation on motor cortex excitability in humans. *The*
472 *Journal of physiology*. 2013;591(7):1987-2000.
- 473 9. Thirugnanasambandam N, Grundey J, Adam K, Drees A, Skwirba AC, Lang N, et al.
474 Nicotinic impact on focal and non-focal neuroplasticity induced by non-invasive brain stimulation
475 in non-smoking humans. *Neuropsychopharmacology : official publication of the American College of*
476 *Neuropsychopharmacology*. 2011;36(4):879-86.
- 477 10. Jamil A, Batsikadze G, Kuo HI, Labruna L, Hasan A, Paulus W, et al. Systematic evaluation of
478 the impact of stimulation intensity on neuroplastic after-effects induced by transcranial direct
479 current stimulation. *The Journal of physiology*. 2017;595(4):1273-88.
- 480 11. Ammann C, Lindquist MA, Celnik PA. Response variability of different anodal transcranial
481 direct current stimulation intensities across multiple sessions. *Brain stimulation*. 2017.
- 482 12. Gabriel C, Gabriel S, Corthout E. The dielectric properties of biological tissues: I. Literature
483 survey. *Physics in Medicine and Biology*. 1996;41(11):2231-49.
- 484 13. Huang Y, Liu AA, Lafon B, Friedman D, Dayan M, Wang X, et al. Measurements and models of
485 electric fields in the in vivo human brain during transcranial electric stimulation. *eLife*. 2017;6.

- 486 14. Lang N, Siebner HR, Ward NS, Lee L, Nitsche MA, Paulus W, et al. How does transcranial DC
487 stimulation of the primary motor cortex alter regional neuronal activity in the human brain? The
488 European journal of neuroscience. 2005;22(2):495-504.
- 489 15. Pena-Gomez C, Sala-Lonch R, Junque C, Clemente IC, Vidal D, Bargallo N, et al. Modulation of
490 large-scale brain networks by transcranial direct current stimulation evidenced by resting-state
491 functional MRI. Brain stimulation. 2012;5(3):252-63.
- 492 16. Datta A, Bansal V, Diaz J, Patel J, Reato D, Bikson M. Gyri-precise head model of transcranial
493 direct current stimulation: improved spatial focality using a ring electrode versus conventional
494 rectangular pad. Brain stimulation. 2009;2(4):201-7, 7 e1.
- 495 17. Dmochowski JP, Datta A, Bikson M, Su Y, Parra LC. Optimized multi-electrode stimulation
496 increases focality and intensity at target. Journal of neural engineering. 2011;8(4):046011.
- 497 18. Wagner T, Fregni F, Fecteau S, Grodzinsky A, Zahn M, Pascual-Leone A. Transcranial direct
498 current stimulation: a computer-based human model study. NeuroImage. 2007;35(3):1113-24.
- 499 19. Teichmann M, Lesoil C, Godard J, Vernet M, Bertrand A, Levy R, et al. Direct current
500 stimulation over the anterior temporal areas boosts semantic processing in primary progressive
501 aphasia. Annals of neurology. 2016;80(5):693-707.
- 502 20. Seibt O, Brunoni AR, Huang Y, Bikson M. The Pursuit of DLPFC: Non-neuronavigated Methods
503 to Target the Left Dorsolateral Pre-frontal Cortex With Symmetric Bicephalic Transcranial Direct
504 Current Stimulation (tDCS). Brain stimulation. 2015;8(3):590-602.
- 505 21. Di Lazzaro V, Profice P, Ranieri F, Capone F, Dileone M, Oliviero A, et al. I-wave origin and
506 modulation. Brain stimulation. 2012;5(4):512-25.
- 507 22. Radman T, Ramos RL, Brumberg JC, Bikson M. Role of cortical cell type and morphology in
508 subthreshold and suprathreshold uniform electric field stimulation in vitro. Brain stimulation.
509 2009;2(4):215-28, 28 e1-3.
- 510 23. Dmochowski JP, Bikson M, Datta A, Richardson J, Fridriksson J, Parra LC. On the role of
511 electric field orientation in optimal design of transcranial current stimulation. Conference
512 proceedings : Annual International Conference of the IEEE Engineering in Medicine and Biology
513 Society IEEE Engineering in Medicine and Biology Society Annual Conference. 2012;2012:6426-9.
- 514 24. Rahman A, Reato D, Arlotti M, Gasca F, Datta A, Parra LC, et al. Cellular effects of acute
515 direct current stimulation: somatic and synaptic terminal effects. The Journal of physiology.
516 2013;591(10):2563-78.
- 517 25. Mills KR, Boniface SJ, Schubert M. Magnetic brain stimulation with a double coil: the
518 importance of coil orientation. Electroencephalography and clinical neurophysiology. 1992;85(1):17-
519 21.
- 520 26. Werhahn KJ, Fong JK, Meyer BU, Priori A, Rothwell JC, Day BL, et al. The effect of magnetic
521 coil orientation on the latency of surface EMG and single motor unit responses in the first dorsal
522 interosseous muscle. Electroencephalography and clinical neurophysiology. 1994;93(2):138-46.
- 523 27. Bikson M, Inoue M, Akiyama H, Deans JK, Fox JE, Miyakawa H, et al. Effects of uniform
524 extracellular DC electric fields on excitability in rat hippocampal slices in vitro. The Journal of
525 physiology. 2004;557(Pt 1):175-90.
- 526 28. Truong DQ, Magerowski G, Blackburn GL, Bikson M, Alonso-Alonso M. Computational
527 modeling of transcranial direct current stimulation (tDCS) in obesity: Impact of head fat and dose
528 guidelines. NeuroImage: Clinical. 2013;2:759-66.
- 529 29. Ashburner J, Friston KJ. Unified segmentation. NeuroImage. 2005;26(3):839-51.
- 530 30. Penny WD, Friston KJ, Ashburner JT, Kiebel SJ, Nichols TE. Statistical Parametric Mapping:
531 The Analysis of Functional Brain Images: Academic Press; 2011 2011/04/28/. 689 p.
- 532 31. Huang Y, Dmochowski JP, Su Y, Datta A, Rorden C, Parra LC. Automated MRI segmentation
533 for individualized modeling of current flow in the human head. J Neural Eng. 2013;10(6):066004.
- 534 32. Yousry TA, Schmid UD, Alkadhi H, Schmidt D, Peraud A, Buettner A, et al. Localization of the
535 motor hand area to a knob on the precentral gyrus. A new landmark. Brain : a journal of neurology.
536 1997;120 (Pt 1):141-57.

- 537 33. Dechent P, Frahm J. Functional somatotopy of finger representations in human primary
538 motor cortex. *Human brain mapping*. 2003;18(4):272-83.
- 539 34. Wagner T, Fregni F, Fecteau S, Grodzinsky A, Zahn M, Pascual-Leone A. Transcranial direct
540 current stimulation: A computer-based human model study. *NeuroImage*. 2007;35(3):1113-24.
- 541 35. Huang Y, Liu AA, Lafon B, Friedman D, Dayan M, Wang X, et al. Measurements and models of
542 electric fields in the in vivo human brain during transcranial electric stimulation. *eLife*.
543 2017;6:e18834.
- 544 36. Kojima S, Onishi H, Miyaguchi S, Kotan S, Sugawara K, Kirimoto H, et al. Effects of cathodal
545 transcranial direct current stimulation to primary somatosensory cortex on short-latency afferent
546 inhibition. *Neuroreport*. 2015;26(11):634-7.
- 547 37. Datta A, Elwassif M, Battaglia F, Bikson M. Transcranial current stimulation focality using disc
548 and ring electrode configurations: FEM analysis. *Journal of neural engineering*. 2008;5(2):163-74.
- 549 38. Miranda PC, Lomarev M, Hallett M. Modeling the current distribution during transcranial
550 direct current stimulation. *Clinical neurophysiology : official journal of the International Federation
551 of Clinical Neurophysiology*. 2006;117(7):1623-9.
- 552 39. Rampersad SM, Janssen AM, Lucka F, Aydin U, Lanfer B, Lew S, et al. Simulating transcranial
553 direct current stimulation with a detailed anisotropic human head model. *IEEE transactions on
554 neural systems and rehabilitation engineering : a publication of the IEEE Engineering in Medicine and
555 Biology Society*. 2014;22(3):441-52.
- 556 40. Jog MV, Smith RX, Jann K, Dunn W, Lafon B, Truong D, et al. In-vivo Imaging of Magnetic
557 Fields Induced by Transcranial Direct Current Stimulation (tDCS) in Human Brain using MRI. *Scientific
558 reports*. 2016;6:34385.
- 559 41. Opitz A, Falchier A, Yan CG, Yeagle EM, Linn GS, Megevan P, et al. Spatiotemporal structure
560 of intracranial electric fields induced by transcranial electric stimulation in humans and nonhuman
561 primates. *Scientific reports*. 2016;6:31236.
- 562 42. Laakso I, Tanaka S, Koyama S, De Santis V, Hirata A. Inter-subject Variability in Electric Fields
563 of Motor Cortical tDCS. *Brain stimulation*. 2015;8(5):906-13.
- 564 43. Bestmann S, Ward N. Are current flow models for transcranial electrical stimulation fit for
565 purpose? *Brain stimulation*. 2017.
- 566 44. Horvath JC, Forte JD, Carter O. Evidence that transcranial direct current stimulation (tDCS)
567 generates little-to-no reliable neurophysiologic effect beyond MEP amplitude modulation in healthy
568 human subjects: A systematic review. *Neuropsychologia*. 2015;66:213-36.
- 569 45. Tremblay S, Hannah R, Rawji V, Rothwell JC. Modulation of iTBS after-effects via concurrent
570 directional TDCS: A
571 proof of principle study. *Brain stimulation*. 2017.
- 572 46. Wiethoff S, Hamada M, Rothwell JC. Variability in response to transcranial direct current
573 stimulation of the motor cortex. *Brain stimulation*. 2014;7(3):468-75.
- 574 47. Li LM, Uehara K, Hanakawa T. The contribution of interindividual factors to variability of
575 response in transcranial direct current stimulation studies. *Frontiers in cellular neuroscience*.
576 2015;9:181.
- 577 48. Gartside IB. Mechanisms of sustained increases of firing rate of neurones in the rat cerebral
578 cortex after polarization: role of protein synthesis. *Nature*. 1968;220(5165):383-4.
- 579 49. Radman T, Su Y, An JH, Parra LC, Bikson M. Spike timing amplifies the effect of electric fields
580 on neurons: implications for endogenous field effects. *The Journal of neuroscience : the official
581 journal of the Society for Neuroscience*. 2007;27(11):3030-6.
- 582 50. Fritsch B, Reis J, Martinowich K, Schambra HM, Ji Y, Cohen LG, et al. Direct current
583 stimulation promotes BDNF-dependent synaptic plasticity: potential implications for motor learning.
584 *Neuron*. 2010;66(2):198-204.
- 585 51. Kuo HI, Bikson M, Datta A, Minhas P, Paulus W, Kuo MF, et al. Comparing cortical plasticity
586 induced by conventional and high-definition 4 x 1 ring tDCS: a neurophysiological study. *Brain
587 stimulation*. 2013;6(4):644-8.

- 588 52. Polania R, Nitsche MA, Paulus W. Modulating functional connectivity patterns and
589 topological functional organization of the human brain with transcranial direct current stimulation.
590 Human brain mapping. 2011;32(8):1236-49.
- 591 53. Lafon B, Rahman A, Bikson M, Parra LC. Direct Current Stimulation Alters Neuronal
592 Input/Output Function. Brain stimulation. 2017;10(1):36-45.
- 593 54. Reato D, Rahman A, Bikson M, Parra LC. Low-intensity electrical stimulation affects network
594 dynamics by modulating population rate and spike timing. The Journal of neuroscience : the official
595 journal of the Society for Neuroscience. 2010;30(45):15067-79.
- 596 55. Lopez-Alonso V, Fernandez-Del-Olmo M, Costantini A, Gonzalez-Henriquez JJ, Cheeran B.
597 Intra-individual variability in the response to anodal transcranial direct current stimulation. Clinical
598 neurophysiology : official journal of the International Federation of Clinical Neurophysiology.
599 2015;126(12):2342-7.

600